

## High Temperature Oxidation Behavior of Flake and Spheroidal Graphite Cast Irons

Meng-Bin Lin · Chaur-Jeng Wang · Alex A. Volinsky

Received: 11 October 2010 / Revised: 2 March 2011 / Published online: 13 March 2011  
© Springer Science+Business Media, LLC 2011

**Abstract** Flake and spheroidal graphite cast irons with similar composition were subjected to high temperature oxidation to investigate graphite morphology and distribution effects on the oxidation behavior. High temperature oxidation tests were conducted between 400 and 750 °C in air. For comparison low carbon steel was also tested. Graphite morphology obviously affected high-temperature oxidation resistance. The flake graphite cast iron exhibited the worst high-temperature oxidation resistance compared with spheroidal graphite cast iron. Since graphite flakes provide suitable sites for the iron oxide growth and are almost interconnected, the iron oxide grows faster and penetrates along the graphite flakes boundaries resulting in the subsurface oxidation. Due to the severe subsurface oxidation flake graphite cast iron parabolic rate constants are five times higher than that of the spheroidal graphite cast iron. However, spheroidal graphite cast iron parabolic rate constants and oxide layer thickness are similar to those of the low carbon steel. Therefore, graphite flakes have negative effect on the cast iron high temperature oxidation resistance.

**Keywords** Flake graphite cast iron · Spheroidal graphite cast iron · High temperature oxidation · Subsurface oxidation

---

M.-B. Lin (✉) · C.-J. Wang  
Department of Mechanical Engineering, National Taiwan University of Science and Technology,  
Taipei 106, Taiwan, ROC  
e-mail: d9603506@mail.ntust.edu.tw

C.-J. Wang  
e-mail: cjwang@mail.ntust.edu.tw

A. A. Volinsky  
Department for Mechanical Engineering, University of South Florida, Tampa,  
FL 33620, USA  
e-mail: volinsky@eng.usf.edu

## Introduction

Flake and spheroidal graphite cast irons have excellent castability, wear resistance, high damping, good machinability and relatively low cost compared with alloy steels with similar mechanical properties. Both irons are used as engineering materials in high temperature applications (ex. furnace parts, exhaust manifolds and turbocharger housings) that require high-temperature corrosion resistance and mechanical strength [1–6].

Cast iron high-temperature oxidation behavior is different from low carbon steel because cast iron contains more carbon leading to graphite precipitation in the ferrite matrix. Above 400 °C graphite is not stable and easy oxidizes in air. Oxidized graphite leaves pores and/or cracks, allowing oxygen inward penetration resulting in further metal oxidation [7–9]. Therefore, it is believed that the cast iron high-temperature oxidation resistance can be influenced by the graphite morphology. However, this subject is not adequately covered in the literature; thus, this study investigates flake and spheroidal graphite cast irons and low carbon steel oxidation behavior between 400 and 750 °C at air. Finally, graphite morphology and distribution effects on the cast iron high-temperature oxidation are discussed.

## Experimental Procedures

Three commercial, fully-annealed materials were used in this study: FC200 flake graphite cast iron, FCD400 spheroidal graphite cast iron and SB450 low carbon steel. Both cast irons were provided by Yongzhen Co., Ltd, Taiwan. Cast iron chemical composition was analyzed by glow discharge spectrometer (LECO, GDS-750A, Germany) as shown in Table 1. The matrix of both cast irons is ferrite and their microstructure is shown in Fig. 1. The specimens were cut into 10 mm×10 mm×2 mm pieces. They were polished with grit paper up to 800 grade and then degreased in an acetone bath, finally cleaned ultrasonically in an ethanol bath, and dried in air before high temperature testing. Specimens were placed in an oven with temperature varied from 400 to 750 °C in air.

After oxidation testing specimens were cooled in air and their mass was measured within 2 min. Oxidized specimens mass was measured with a microbalance, and the value of weight change per unit area was averaged from four specimens under each experimental condition. Specimens' microstructure after oxidation was investigated by means of optical microscopy (OM), scanning electron

**Table 1** Chemical composition of the flake and spheroidal graphite cast irons and low carbon steel (wt%)

Alloy	C	Si	Mn	P	S	Cr	Ni	Mo	Cu	Fe
FC200	2.95	1.53	1.01	0.04	0.01	0.19	0.03	0.05	0.08	Balance
FCD400	2.22	2.55	0.24	0.01	0.00	0.15	0.02	0.04	0.01	Balance
SB450	0.10	0.08	1.37	0.02	0.00	0.01	0.01	0.05	0.00	Balance

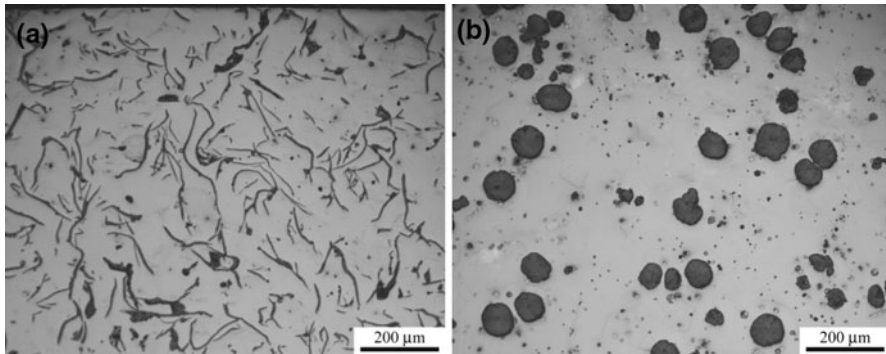


**Fig. 1** Cast iron micrographs: **a** FC200 flake graphite cast iron (ferrite matrix and graphite flakes); **b** FC400 spheroidal graphite cast iron (ferrite matrix and graphite spheroids)

microscopy (SEM) equipped with energy-dispersive X-ray spectrometer (EDS) and X-ray diffractometry (XRD).

## Results and Discussion

### Temperature Effects on Cast Iron and Low Carbon Steel Oxidation Behavior

Figure 2a–c shows oxidation kinetics of the flake graphite, spheroidal graphite and low carbon steel exposed to 400–750 °C in air for 4–192 h. The weight of both kinds of cast iron slightly increased with oxidation time at 400 °C, while it decreased with oxidation time increasing to 48 h accompanied with weight loss. However, low carbon steel specimens' weight always increased with oxidation time. This means that cast iron and low carbon steel oxidation mechanisms are different. The oxidation mechanism of cast iron consists of two reactions: iron oxidation ( $x\text{Fe} + y\text{O} \rightarrow \text{Fe}_x\text{O}$ ) and graphite oxidation ( $2\text{C} + \text{O}_2 \rightarrow 2\text{CO}$  or  $\text{C} + \text{O}_2 \rightarrow \text{CO}_2$ ) [10]. The first reaction caused iron oxides growth resulting in the specimens' weight gain. The second reaction led to the graphite oxidation resulting in the specimens' weight loss. Cast iron high temperature oxidation kinetics is controlled by iron and graphite oxidation. Thus, the results of cast iron specimens' weight change are the net effects of those two reactions.

It was found that the cast iron oxidation mechanism varies and depends on the oxidation temperature. In the 400–500 °C temperature range iron oxidation reaction is quite slow but the graphite oxidation reaction is fast. In this temperature range cast iron oxidation kinetics is dominated by graphite oxidation. Thus cast iron specimens' weight change at 400–500 °C was negligible and even exhibited weight loss as shown in Fig. 2a and b. Iron parabolic rate constants increased when temperature was elevated to 600 °C. At 600 °C cast iron oxidation kinetics is dominated by iron oxidation opposite to graphite oxidation. Therefore, specimens' weight significantly increased.

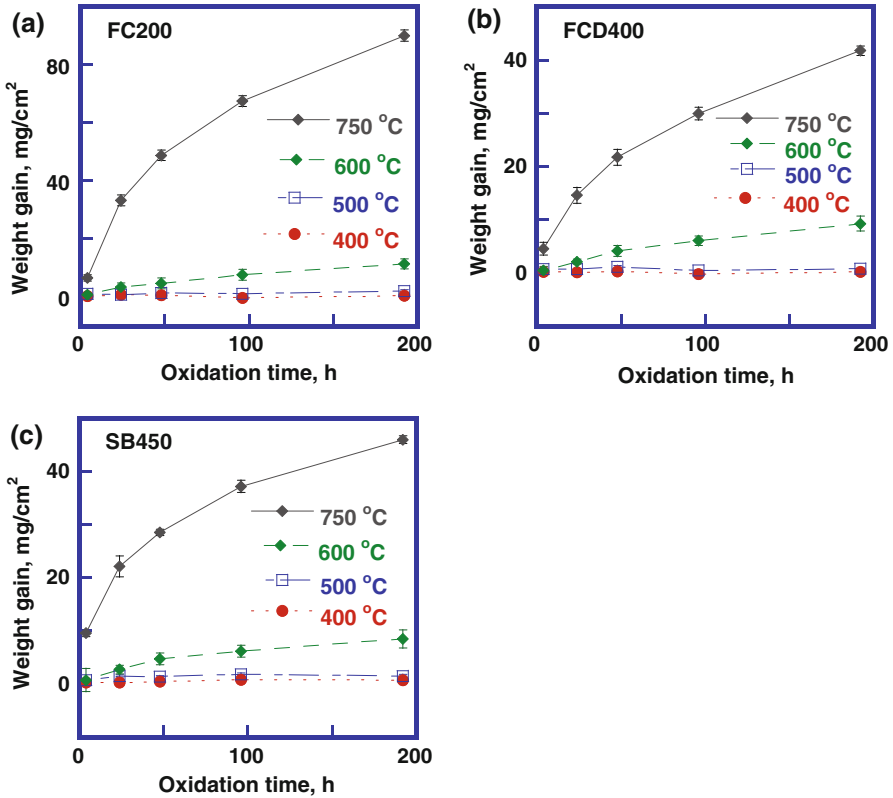


**Fig. 2** Oxidation kinetics between 400 and 750 °C: **a** flake graphite cast iron; **b** spheroidal graphite cast iron and **c** low carbon steel

Figure 2a–c shows that the oxidation mechanism follows the parabolic law. The parabolic rate constants ( $k_p$ ) of samples annealed at 600 °C and 750 °C are listed in Table 2. There is no obvious difference between the three tested materials parabolic rate constants below 600 °C. However, flake graphite cast iron exhibited inferior oxidation resistance compared with spheroidal graphite cast iron and low carbon steel when the oxidation temperature was elevated to 750 °C. Flake graphite cast iron parabolic rate constant at 750 °C is 5 times greater than spheroidal graphite cast iron parabolic rate constant. Spheroidal graphite cast iron parabolic rate constants is essentially equal to that of low carbon steel as shown in Table 2.

**Table 2** Parabolic rate constants for the oxidation of flake, spheroidal graphite cast irons and low carbon steel

Alloy	600 °C $\text{mg}^2 \text{cm}^{-4} \text{s}^{-1}$	750 °C $\text{mg}^2 \text{cm}^{-4} \text{s}^{-1}$
FC200	$2.3 \times 10^{-4}$	$13.45 \times 10^{-3}$
FCD400	$1.4 \times 10^{-4}$	$2.70 \times 10^{-3}$
SB450	$1.2 \times 10^{-4}$	$2.50 \times 10^{-3}$

## Oxide Layers Microstructure and Phase Composition

BEI micrographs of cross sections of flake graphite cast iron, spheroidal graphite cast iron and low carbon steel after oxidation testing at 750 °C for 24 h are presented in Fig. 3a–c. Extensive oxidation of FC200 was observed; the oxide layer of FC200 exhibits thicker and porous morphology compared with that of FCD400 and SB450.

Specimens were gradually ground and XRD phase analysis was performed in-between grinding steps. XRD results are shown in Fig. 3d, which indicates that the oxide layers of these three material are consistent with  $\text{Fe}_2\text{O}_3$  surface layer,  $\text{Fe}_3\text{O}_4$  and  $\text{FeO}$  inner layers.

According to the Fe–O phase diagram  $\text{FeO}$  only exists above 570 °C and grows much faster than other oxides [11]. Therefore, severe iron oxidation above 570 °C promoted thicker iron oxide layer growth resulting in significant specimens' weight gain. It is noticeable that  $\text{FeO}$  in the flake graphite cast irons obviously exhibited the subsurface growth behavior and propagated along the graphite boundary, as seen in Fig. 3a. This is different from the  $\text{FeO}$  outward growth behavior in pure iron, where  $\text{FeO}$  grows as a result of the iron ions outward diffusion [12]. The difference may be caused by the existence of graphite flakes. At high temperature oxygen penetrates into material through the graphite flakes boundaries. The formation and growth of  $\text{FeO}$  in the inner subsurface is promoted by oxygen penetration through graphite boundaries with the ferrite matrix.

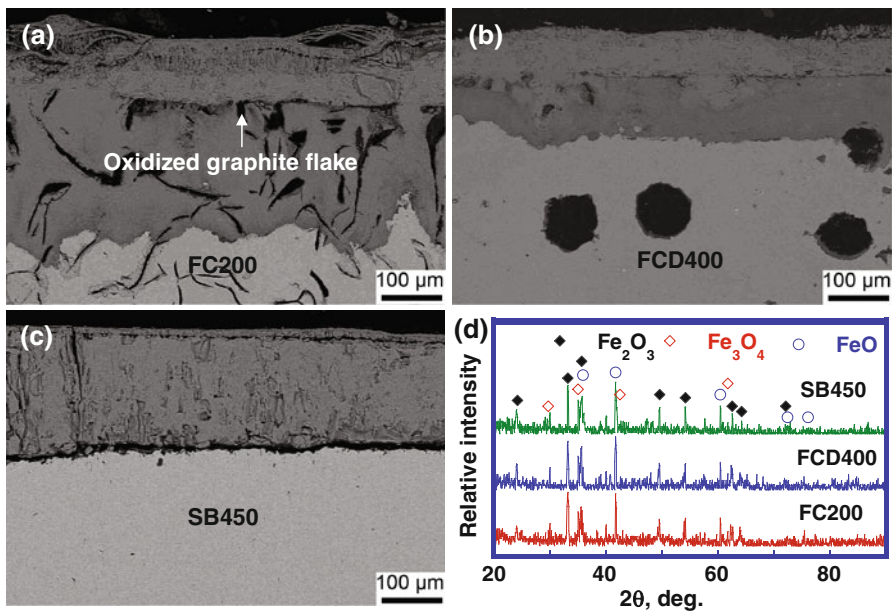


**Fig. 3** BEI micrographs of cross sections of oxide layers and XRD analysis: **a** Flake graphite cast iron; **b** spheroidal graphite cast iron; **c** low carbon steel, after 750 °C oxidation test for 24 h; **d** X-ray diffraction pattern from oxide layer revealing  $\text{Fe}_2\text{O}_3$ ,  $\text{Fe}_3\text{O}_4$  and  $\text{FeO}$  phases

Since the oxide layer microstructure and substrate chemical composition of flake and spheroidal graphite irons are similar, it is reasonable to assume that the high temperature oxidation resistance of flake graphite cast iron is inferior to spheroidal graphite cast iron due to the graphite morphology and distribution.

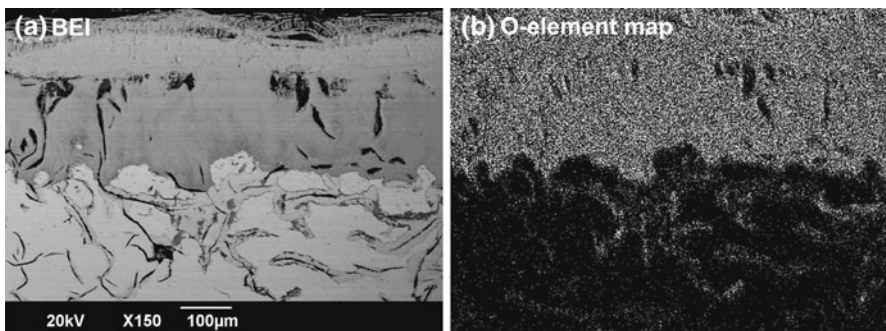
#### Graphite Morphology Effect on Cast Iron High Temperature Oxidation Behavior

Figure 4a and b show flake graphite cast iron backscattered electrons image and O element map after 750 °C oxidation for 24 h. O element map of flake graphite cast iron exposed to 750 °C for 24 h (Fig. 4b) provides evidence that the graphite-iron boundaries are good diffusion paths for oxygen diffusing inside. Since the graphite oxidation is spontaneous at 750 °C, graphite would be oxidized and provide oxygen diffusion path along the graphite oxide boundaries [12]. The oxidized graphite would leave cracks and pores resulting in oxygen penetration into iron promoting iron oxide growth [13]. As shown in Fig. 4a, iron oxides had formed and penetrated along the boundaries between the graphite and the iron matrix.

Therefore, the morphology and distribution of graphite is considered the most significant to dominate the high temperature cast iron oxidation resistance. In this study carbon content and the ferrite matrix in tested cast irons is the same, so the amount of graphite in both cast irons should be similar. However, the graphite morphology and distribution in cast iron would determine the oxidation path.

The mechanism of graphite flakes growth is planar resulting in extended and dispersed morphology in the cast iron [14], as seen in Fig. 1a. Meanwhile spheroidal graphite growth mechanism is three-dimensional. Thus, spheroidal graphite does not provide continuous graphite dispersion, as seen in Fig. 1b. Due to the flake graphite cast iron planar growth, graphite flakes provide almost continuous path for the iron oxide propagation. Thus it is reasonable to believe that as flake graphite cast iron oxidizes in high temperature environment, iron oxides grow and penetrate along the graphite flakes resulting in severe subsurface oxidation.

Figure 5 shows optical micrographs of the flake graphite cast iron after 750 °C air oxidation test for various exposure times revealing severe sub-surface oxidation. The oxide layer had formed and penetrated into the substrate along the graphite



**Fig. 4** a Backscattered electron image and b O-element map of the flake graphite cast iron oxide layer after 750 °C 24 h oxidation test

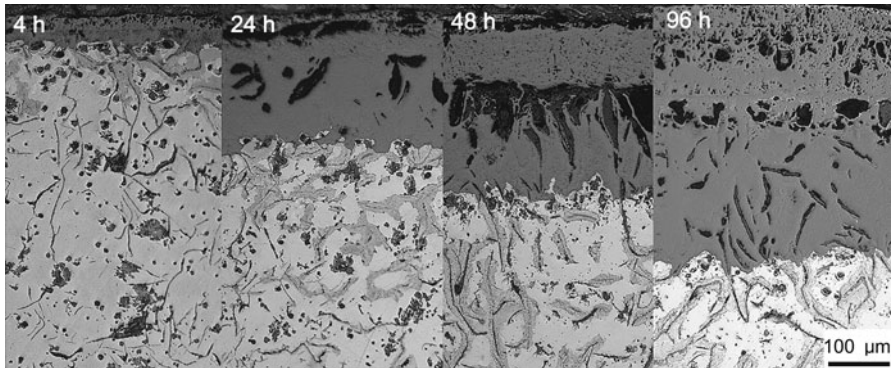


**Fig. 5** Optical micrograph of oxide layer growth behavior of flake graphite cast iron exposed to 750 °C in air for 4–96 h. Oxygen penetrated along flake graphite boundaries led to iron oxide subsurface growth

flakes/ferrite matrix boundaries after 4 h 750 °C exposure. Although the oxide layer formed, it contains large porosity caused by extensive graphite flakes oxidation (Fig. 5, exposed for 24 h) resulting in further oxygen attack. Consequently, the rate of oxide layer growth of flake graphite cast iron is significantly higher than that of spheroidal graphite cast iron and low carbon steel. Finally, iron oxides thickness grew in the subsurface and propagated fast along the graphite flakes boundaries with increasing exposure time from 4 h to 96 h, as seen in Fig. 5. Due to severe iron oxide subsurface growth taking place in flake graphite cast iron, it exhibits much higher parabolic rate constants and thicker iron oxide layer than spheroidal graphite cast iron.

It was confirmed that iron oxide subsurface growth behavior did not take place in the spheroidal graphite cast iron during high temperature oxidation tests. Besides, parabolic rate constants of spheroidal graphite cast iron and low carbon steel are similar. Thus, it is reasonable to assume that spheroidal graphite cast iron is better suited for high temperature applications than flake graphite cast iron due to the structure and distribution of graphite spheroids not providing continuous oxygen path suppressing iron oxides growth.

## Conclusions

This study revealed that the flake graphite cast iron exhibited worse high-temperature oxidation resistance than the spheroidal graphite cast iron and low carbon steel. Since graphite flakes provide suitable sites for iron oxides growth and the flakes are almost interconnected, iron oxides grow fast and penetrate along the graphite flakes/ferrite matrix boundaries resulting in the subsurface oxidation. Due to the severe subsurface oxidation the overall parabolic rate constants is 5 times higher for the flake graphite cast iron compared with the spheroidal graphite cast iron when temperature is elevated to 750 °C. However, spheroidal graphite cast iron parabolic rate constants and the iron oxide layer thickness are similar to

that of the low carbon steel. Therefore, graphite flakes have a negative effect on the cast iron high-temperature oxidation resistance.

**Acknowledgments** The authors acknowledge support from the National Science Council of Republic of China under grant NSC 98-2221-E-011-038. Alex Volinsky would like to acknowledge support from the National Science Foundation.

## References

1. C. Labrecque and M. Gagne, *Canadian Metallurgical Quarterly* **37**, 343 (1998).
2. P. Curcio, B. Kerezi, and P. Brown, *Journal of Materials Science* **34**, 4775 (1999).
3. G. S. Cho, K. H. Choe, K. W. Lee, and A. Ikenaga, *Journal of Materials Science and Technology* **23**, 97 (2007).
4. A. R. Ghaderi, M. Nili Ahmadabadi, and H. M. Ghasemi, *Wear* **225**, 410 (2003).
5. M. Hatate, T. Shoita, N. Takahashi, and K. Shimizu, *Wear* **251**, 885 (2001).
6. Y. Zhang, Y. Chen, R. He, and B. Shen, *Wear* **166**, 179 (1993).
7. T. Ban, *Corrosion Science* **19**, 1979 (289).
8. F. Tholence, *Surface Interface Analysis* **34**, 535 (2002).
9. A. Atkinson, *Corrosion Science* **22**, 87 (1982).
10. J. Robertson and M. I. Manning, *Materials Science and Technology* **5**, 741 (1989).
11. A. S. Khanna, *High Temperature Oxidation and Corrosion* (ASM International, 2002), p. 84.
12. P. Kofstad, *Nonstoichiometry, Diffusion and Electrical Conductivity in Binary Metal Oxides*, (Wiley-Interscience, New York, 1972).
13. D. R. Gaskell, *Introduction to the Thermodynamics* (McGraw-Hill International, New York), p. 585.
14. D. D. Double and A. Hellowell, *Acta Metallurgica* **22**, 481 (1974).